Roles of Crustacean Female Sex Hormone 1a in a Protandric Simultaneous Hermaphrodite Shrimp

Fang Liu[1], Wenyuan Shi[2], Lin Huang[2], Guizhong Wang[2], Zhihuang Zhu[3] and Haihui Ye[1]*

[1] College of Fisheries, Jimei University, Xiamen, China, [2] College of Ocean and Earth Sciences, Xiamen University, Xiamen, China, [3] Fisheries Research Institute of Fujian, Xiamen, China

Crustacean female sex hormone (CFSH) plays a pivotal role in the development of secondary sex characteristics in dioecious crustaceans. However, until now the knowledge concerning its functions in hermaphroditic species is scanty. Herein, we explored the function of CFSH (*Lvit-CFSH1a*) in the peppermint shrimp *Lysmata vittata*, a species characterized by a rare reproductive system of protandric simultaneous hermaphroditism (PSH). *Lvit-CFSH1a* cDNA was 1,220-bp in length with a 720-bp ORF encoded a polypeptide of 239-aa. RT-PCR showed that *Lvit-CFSH1a* was exclusively expressed in the eyestalk ganglion. For female physiology, it was found that *Lvit*-CFSH1a was indispensable for the development of female gonopores, but it might not involve vitellogenesis of the species. For male physiology, *Lvit*-CFSH1a suppressed *Lvit-IAG2* expression in short-term silencing experiment and recombinant protein injection experiment, but did not affect male sexual differentiation in long-term silencing experiment. In addition, silencing the *Lvit-CFSH1a* gene impeded individual growth in *L. vittata*.

Keywords: sexual differentiation, CFSH, PSH, reproductive endocrine, crustaceans

INTRODUCTION

Gonochorism is the most common reproductive strategy in decapod crustacean species (Juchault, 1999). In dioecious decapod crustaceans, androgenic gland hormone (AGH) and insulin-like androgenic gland hormone (IAG) secreted mainly by androgenic gland (AG), play critical roles in sexual differentiation (Manor et al., 2007). Implantation of AG into females induced masculinization in the red swamp crayfish *Procambarus clarkii* (Taketomi and Nishikawa, 1996), the giant freshwater prawn *Macrobrachium rosenbergii* (Nagamine et al., 1980; Malecha et al., 1992) and the red claw crayfish *Cherax quadricarinatus* (Khalaila et al., 2001; Barki et al., 2003), and vice versa (Barki et al., 2006). Likewise, silencing of IAG genes in males blocked male sexual differentiation while stimulating feminization. For instance, knockdown of *IAG* led to the arrest of testicular spermatogenesis and incomplete development of secondary sexual characteristics (appendices masculinae) in young *M. rosenbergii* males (Ventura et al., 2009). Moreover, silencing IAG gene could also feminize male-related phenotypes in the intersex *C. quadricarinatus* (Rosen et al., 2010) and the male Chinese mitten crab *Eriocheir sinensis* (Fu et al., 2020), and even induce fully sex reversal in young *M. rosenbergii* males (Ventura et al., 2009). Therefore, by virtue of its universal role as a master regulator of crustacean male development, IAG was also termed the

sexual "IAG-switch" (Levy and Sagi, 2020). It was presumed that females arose as the absence of AG or IAG (Ventura et al., 2009).

In 2014, Zmora and Chung (2014) identified a neurohormone from the eyestalk ganglion in the Atlantic blue crab *Callinectes sapidus*. The neurohormone was named crustacean female sex hormone (CFSH) as its pivotal roles in the development of the female's mating and egg brooding systems, including the gonopores and ovigerous setae (Zmora and Chung, 2014). In recent years, more and more full-length transcripts for CFSH orthologs have also been found in decapod crustacean species (Ventura et al., 2014; Veenstra, 2015, 2016; Nguyen et al., 2016; Kotaka and Ohira, 2018; Liu et al., 2018; Tsutsui et al., 2018; Thongbuakaew et al., 2019). Interestingly, CFSH genes were not exclusively expressed in the eyestalk ganglion in certain numbers of crustacean species (Veenstra, 2015; Nguyen et al., 2016; Tsutsui et al., 2018; Thongbuakaew et al., 2019). For instance, *MroCFSH1a* was specifically identified in the central nervous system (CNS), ovary, and testis; while *MroCFSH2b* was expressed in various tissues excluding heart, and muscle (Thongbuakaew et al., 2019). It was also noteworthy that more than one CFSH transcripts were identified in some species (Veenstra, 2015, 2016; Kotaka and Ohira, 2018; Tsutsui et al., 2018; Thongbuakaew et al., 2019). Such examples were shown in *P. clarkii* (*Prc-CFSH*, *Prc-CFSH-like 1,* and *Prc-CFSH-like 2*) (Veenstra, 2015), *E. sinensis* (*Esi-CFSH1*, *Esi-CFSH2a,* and *Esi-CFSH2b*) (Veenstra, 2016) and *M. rosenbergii* (*MroCFSH1a*, *MroCFSH1b*, *MroCFSH2a,* and *MroCFSH2b*) (Thongbuakaew et al., 2019). Interestingly, the expression levels of CFSH showed no significant difference between males and females in the eastern rock lobster *Sagmariasus verreauxi* (Ventura et al., 2014), and similar phenomenon was observed in prepubertal individuals of the mud crab *Scylla paramamosain* (Liu et al., 2018). Even so, function studies of CFSHs were demonstrated only in a few dioecious crustacean species (Liu et al., 2018; Tsutsui et al., 2018; Thongbuakaew et al., 2019; Jiang et al., 2020). In the mud crab *S. paramamosain*, CFSH not only regulated sexual differentiation of early juveniles (Jiang et al., 2020), but also acted as an inhibitor of IAG in prepubertal males (Liu et al., 2018). In the kuruma prawn *Marsupenaeus japonicus*, *Maj-CFSH-ov*, which was dominantly expressed in the ovary, might be involved in some reproductive process other than vitellogenesis (Tsutsui et al., 2018). However, *Mro*CFSHs were suggested to be involved in vitellogenesis induced by 5-hydroxytryptamine (5-HT) addition in ovary explants of *M. rosenbergii* (Thongbuakaew et al., 2019).

Interestingly, a review of the literature shows that Caridean shrimps exhibit several other protandry sexual systems apart from gonochorism (Bauer, 2000). To date, however, there are rare reports elaborating sexual differentiation mechanism in protandric crustaceans. In the strictly sequential protandric hermaphroditism (SPH) shrimp *Pandalus platyceros*, *Pnp-IAG* knockdown elevated the expression of *vitellogenin* in the hepatopancreas and promoted transformation of the gonad from ovotestis to ovary (Levy et al., 2020). In the protandric simultaneous hermaphroditism (PSH) shrimp *Lysmata wurdemanni*, it was suggested that IAG was possibly

responsible for the maintenance of the male reproductive activity in euhermaphrodite phase (Zhang et al., 2017). More detailed studies were performed in another PSH shrimp *L. vittata*. It was demonstrated that *Lvit-IAG1* and *Lvit-IAG2* jointly regulated male sexual differentiation (Liu et al., 2021a,b). Meanwhile, *Lvit-IAG1* was also suggested to regulate the ovarian development by inhibiting *Lvit-GIHs* expression (Liu et al., 2021b). Recently, two CFSH transcripts (*Lvit-CFSH1a* and *Lvit-CFSH1b*) have been identified from *L. vittata* by transcriptomic analysis (Bao et al., 2020), however, no further in-depth studies are conducted.

In this study, we explored the function of *Lvit*-CFSH1a in *L. vittata*, a species that displays the unique PSH sexual system, whereby individuals first mature as males; and then, with increasing age and size, acquire reproductive functions of both males and females (Bauer, 2000; Alves et al., 2019). Considering that CFSH acts as an inhibitor of IAG (Liu et al., 2018), we hypothesized that *Lvit*-CFSH1a not only regulated female sexual differentiation, but also involved male sexual differentiation via inhibiting *Lvit-IAGs* expression of the PSH species. To validate this hypothesis, we performed both short-term and long-term gene knockdown via RNA interference (RNAi). In addition, we expressed recombinant *Lvit*-CFSH1a mature peptide (r*Lvit*-CFSH1a) using a prokaryotic expression system, and carried out *in vivo* experiment to examine the effect of *Lvit*-CFSH1a on the expression of *Lvit-IAG1*, *Lvit-IAG2*, *Lvit-Vg*, and *Lvit-VgR*.

MATERIALS AND METHODS

Animals

The experimental animals (*L. vittata*) were artificial-bred at the Fisheries Research Institute of Fujian Province, in Xiamen, China. After transport to the laboratory, shrimps were acclimated in seawater aquaria at temperature of $26 \pm 1°C$ and salinity of 32 ± 1 PSU for 2 days. During that period, they were fed with a commercially formulated shrimp diet daily. Two developmental phases covering four gonadal development stages were defined and described for *L. vittata* according to the previous research (Chen et al., 2019).

cDNA Cloning of *Lvit-CFSH1a*

Total RNA was extracted from the eyestalk ganglion of shrimps at gonadal development stage III using TRIzol® reagent (Invitrogen) according to the manufacturer's instructions. The first-strand cDNA for fragment and 3′-untranslated region (3′ UTR) cloning was generated with 1 μg total RNA using RevertAid First Strand cDNA Synthesis Kit (Fermentas). Fragment of *Lvit-CFSH1a* was obtained from a *de novo* transcriptomic library of *L. vittata* and polymerase chain reaction (PCR) by primer pair (CFSH1aF/CFSH1aR) was performed to verify its accuracy. Seminested PCR was performed for 3′ UTR cloning. The 5′ UTR of *Lvit-CFSH1a* was obtained by a method of rapid amplification of cDNA ends (RACE) with SMART™ RACE cDNA Amplification Kit (Clontech) according to the manufacturer's protocol. Primers used in cDNA cloning were list in **Table 1**.

Genomic DNA Amplification of *Lvit-CFSH1a*

EasyPure® Marine Animal Genomic DNA Kit (TransGen) was used to extract the genomic DNA from the eyestalk ganglion of *L. vittata* at gonadal development stage III. Specific primers were designed for amplification of *Lvit-CFSHs* genomic DNA (gDNA) (**Table 1**). The PCR reaction was performed with LA-Taq polymerase (TaKaRa) under the following conditions: 95°C for 5 min; 35 cycles of 95°C for 30 s, 60°C for 30 s, and 72°C for 2 min, followed by 72°C for 10 min final extension.

The Quantitative Real-Time PCR Assays

Primers used for quantitative real-time PCR (qRT-PCR) were from previous studies (Liu et al., 2021a,b). Amplification efficiency of each primer pair was determined before used for qRT-PCR assays. The cDNA was diluted fourfolds using RNase-free water before it was utilized in qRT-PCR detection. Components including, 10 μl TB Green Premix Ex Taq II (2X) (TaKaRa), 2 μl diluted cDNA, 0.5 μl forward/reverse primer (10 μM), as well as and 7 μl RNase-free water, were used for a 20 μl qRT-PCR reaction system. The reaction was performed using in 7500 Real-Time PCR (Applied Biosystems): 95°C for 30 s, followed by 40 cycles of 95°C for 15 s, 58.5°C for 15 s and 72°C for 30 s. The result was calculated using $2^{-\Delta\Delta Ct}$ method, whereby *Lvit*-β-*actin* (GenBank accession number: MT114194) was utilized as the reference gene.

TABLE 1 | Summary of primers used in this study.

Primer	Sequence (5′–3′)	Application
CFSH1aF	CCTTAGCTCAGCAGCAGGGTGT	Fragment validation
CFSH1aR	GGCGGCAGTTCCTTCGTCA	
UPM	CTAATACGACTCACTATAGG GCAAGCAGTGGTATCAACGCAGAGT	5′RACE
5CFSH1aout	GCCTCGGCTCTCCATTTGATGTGCT	
5CFSH1ain	GGGTATGGAGCCGGAAGGTCCAGGTCA	
3adaptor	AAGCAGTGGTATCAACGCAGAGTAC TTTTTTTTTTTTTTTTTTTTTTTTTVN	3′RACE
3GSP	AAGCAGTGGTATCAACGCAGAG	
3CFSH1ain	GGATGAACCTCCACAGGAACCACG	
3CFSH1aout	CATACCCGAAGCCCTTCTTCCTGC	
gCFSH1aF	ATATAGCGACACAAGAAACTCCACC	cDNA/gDNA validation
gCFSH1aR	TGATGAGTCATTTTTATTGGATAATTGA	
CFSH1adsF	TGGCTCCACATCGACCACCGA	dsRNA synthesis
CFSH1adsR	ATCATCGCCGTCCTTGTTCCTCTTC	
GFPdsF	TGGGCGTGGATAGCGGTTTG	
GFPdsR	GGTCGGGGTAGCGGCTGAAG	
T7primer	TAATACGACTCACTATAGGG	
SP6primer	ATTTAGGTGACACTATAG	
SP6primer	ATTTAGGTGACACTATAG	
CFSH1ayhF	CCGGAATTCCCGAACAAGG ACGGCGATGATGAGCTCG	Prokaryotic expression
CFSH1ayhR	CTAGCTAGCCTAGTTTTGTA CAGCGGCAGCGAAGACG	

Tissue Expression of *Lvit-CFSH1a* in *L. vittata*

The total RNA was extracted from various tissues (eyestalk ganglion, brain, thoracic ganglion, abdominal ganglion, ovary, testis, androgenic gland, hepatopancreas, stomach, intestine, heart, gill, and muscle) as described in section "cDNA Cloning of *Lvit-CFSH1a*." The first-strand cDNA was produced from 1 μg total RNA using PrimeScript™ RT reagent Kit with gDNA Eraser (Perfect Real Time) (TaKaRa). Tissue expression profile was determined by RT-PCR under the following conditions: 95°C for 5 min; 35 cycles of 95°C for 30 s, 58.5°C for 30 s, and 72°C for 30 s, followed by 72°C for 5 min final extension. Meanwhile, *Lvit*-β-*actin* (GenBank accession number: MT114194) was amplified as a positive control. RT-PCR products were examined using 1.5% agarose gel imaged by UV detector (Geldoc, Thermo Fisher Scientific).

Expression Profile of *Lvit-CFSH1a* During Gonadal Development

In order to examine expression profile of *Lvit-CFSH1a* during gonadal development, total RNA was extracted from eyestalk ganglion of *L. vittata* at different gonadal development stages (*n* = 5). It was followed by the synthesis of cDNA as described in section "Tissue Expression of *Lvit-CFSH1a* in *L. vittata*" and qRT-PCR detection as described in section "The Quantitative Real-Time PCR Assays," respectively.

dsRNA Preparation

Fragment of *Lvit-CFSH1a* and green fluorescent protein gene (*GFP*) (exogenous gene control) were cloned into pGEM-T Easy Vector (Promega). dsRNA synthesis was performed using T7 RNA Polymerase (Takara) and SP6 RNA Polymerase (TaKaRa) according to standard protocols. Finally, dsRNA was diluted with 10 mM phosphate-buffered saline (PBS, pH 7.4).

Short-Term Silencing Experiment *in vivo*

To evaluate the efficacy of gene knockdown via RNA interference (RNAi), a short-term silencing experiment was carried out with *L. vittata* at gonadal development stage I. A total of 15 shrimps (carapace length 2.99 ± 0.10 mm, body weight 42.79 ± 4.28 mg) were randomly and equally assigned to following 3 treatment groups (*n* = 5): dsRNA *Lvit-CFSH1a*-injected, dsRNA *GFP*-injected and PBS-injected. dsRNA (2 μg/g) (Liu et al., 2021a,b) was delivered via intramuscular injection in the abdominal segment of shrimp. Meanwhile, the PBS-injected group received an equivalent volume of PBS. Sampling was performed 24 h after injection (Shi et al., 2020). Following anesthesia on ice for 5 min, eyestalk ganglion (EG) and androgenic gland (AG) were collected to test the effect of dsRNA-mediated silencing on the specific genes by qRT-PCR. While RNA extraction and qRT-PCR were performed as described above in sections " cDNA Cloning of *Lvit-CFSH1a*" and "The Quantitative Real-Time PCR Assays," the first-strand cDNA was generated with 200 ng total RNA by TransScript® II One—Step gDNA Removal and cDNA short SuperMix Kit (TransGen).

Long-Term Silencing Experiment *in vivo*

A long-term silencing experiment was conducted to determine the potential roles played by *Lvit-CFSH1a* in sexual differentiation and gonadal development. Shrimps (carapace length 3.12 ± 0.17 mm, body weight 47.80 ± 6.42 mg) at gonadal development stage I were randomly divided into three groups ($n = 13$) as described in section "Short-Term Silencing Experiment *in vivo*." Similar dose of dsRNA ($2 \mu g/g$) or equal volume of PBS was injected into the abdominal segment of shrimp once every 4 days for a total of 8 injections in 29-days duration during which shrimps were kept in seawater aquaria under the following conditions: temperature, $26 \pm 1°C$; salinity, 32 ± 1 PSU; 12L:12D photoperiod. On day 30 (24 h after the 8th injection), all of the shrimp were sampled after anesthetization on ice (Shi et al., 2020). Measurements of carapace length and body weight were recorded. Changes in external sexual features and gonadal development were assessed and recorded as described in our laboratory (Liu et al., 2021a,b). Samples of eyestalk ganglion, androgenic gland, ovarian region of the gonad and hepatopancreas were collected to test the effect of long-term silencing on *Lvit-CFSH1b* (GenBank accession number: MT114198), *Lvit-IAG1* (GenBank accession number: MT114196), *Lvit-IAG2* (GenBank accession number: MT114197), *Lvit-Vg* (GenBank accession number: MT113122) and *Lvit-VgR* (GenBank accession number: MT114195) by qRT-PCR. RNA extraction, the first-strand cDNA synthesis, qRT-PCR were also performed as described in section "Short-Term Silencing Experiment *in vivo*." The remaining gonad tissue was fixed in modified Bouin's fixative (25 ml 37–40% formaldehyde, 75 ml saturation picric acid and 5 ml glacial acetic acid) at 4°C for 24 h, followed by gradient alcohol dehydration, paraffin embedding, preparation of 6 μm sections and staining with hematoxylin and eosin (H & E) for histological observation.

In vivo Effect of *rLvit-CFSH1a* on Gene Expression

r*Lvit*-CFSH1a was expressed using a prokaryotic expression system and purified by immobilized metal-affinity chromatography (IMAC) (Bornhorst and Falke, 2000). The fragment encoding the mature peptide of *Lvit*-CFSH1a was cloned into pET-His vector with restriction enzyme sites (*Eco*RI and *Nhe*I). The generated constructs (pET-His-CFSH1a) was transformed into *E. coli TransB* (DE3) and induced at 16°C after adding isopropyl-beta-D-thiogalactopyranoside (IPTG, 0.2 mM final concentration). After 20 h, bacterial cells were harvested by centrifugation. Because r*Lvit*-CFSH1a expressed as inclusion bodies (**Supplementary Figure 1A**), purification was performed under denaturing conditions (8M urea) with Ni Sepharose^{TM} 6 Fast Flow (GE Healthcare) according to the manufacturer's instructions (**Supplementary Figure 1B**). Purified r*Lvit*-CFSH1a was renatured by graded urea dialysis and confirmed by Western blot analysis. Samples were separated by 12% SDS-PAGE gel electrophoresis. The electrophoresed proteins were transferred to a PVDF membrane and blocked with 5% bull serum albumin (BSA)-PBS for 1 h at room temperature. Following blocking, the membrane was washed three times with PBS. After that, it was incubated in ProteinFind® Anti-His Mouse Monoclonal Antibody (1:2,000, TransGen) for 1 h at 37°C. Horseradish peroxidase activity was detected with Western Blotting Mouse IgG DAB Chromogenic Reagent Kit (incubated with Goat Anti-Mouse IgG/HRP, 1:4,000, 1 h, 37°C; Solarbio) according to the manufacturer's instructions.

A total of 10 shrimps (carapace length 5.17 ± 0.22 mm, body weight 179.02 ± 29.41 mg) at gonadal development stage II were randomly and equally assigned to following 2 treatment groups ($n = 5$): r*Lvit*-CFSH1a-injected and PBS-injected. r*Lvit*-CFSH1a ($2 \mu g/g$) was delivered via intramuscular injection in the abdominal segment of shrimp. Meanwhile, the PBS-injected group received an equivalent volume of PBS. Sampling was performed 24 h after injection. After shrimps were anesthetized on ice for 5 min, AG, ovarian region and hepatopancreas were obtained to test the effect of r*Lvit*-CFSH1a-injection on the specific genes by qRT-PCR. RNA extraction, the first-strand cDNA synthesis, qRT-PCR were also performed as described in section "Short-Term Silencing Experiment *in vivo*."

Bioinformatics Analyses

The primers used for cDNA cloning, gDNA cloning, dsRNA preparation and prokaryotic expression were designed with Primer 5.0. The open reading frame (ORF) was predicted by ORF Finder software[1]. We adopted the SignalP-5.0 Server[2] to predict the signal peptides, whereas cysteine residues and putative disulfide bonds were predicted via DiANNA 1.1 web server[3]. Further, sequence alignment of deduced amino acid sequences with reported sequences was performed using the Clustal Omega website[4]. N-glycosylation motif was predicted by NetNGlyc 1.0 Server[5].

The Maximum Likelihood method with 1000 bootstrap replicates based on the JTT matrix-based model in MEGA7 was applied to generate a phylogenetic tree entailing the deduced amino acid sequence of decapoda CFSH mature peptides. Most of CFSH sequences were borrowed from previous works (Thongbuakaew et al., 2019); other sequences were shown in **Table 2**.

---

[1]https://www.ncbi.nlm.nih.gov/orffinder/
[2]http://www.cbs.dtu.dk/services/SignalP/
[3]http://clavius.bc.edu/~clotelab/DiANNA/
[4]https://www.ebi.ac.uk/Tools/msa/clustalo/
[5]http://www.cbs.dtu.dk/services/NetNGlyc/

TABLE 2 | Summary of sequences used in multiple sequence alignment and phylogenetic analysis.

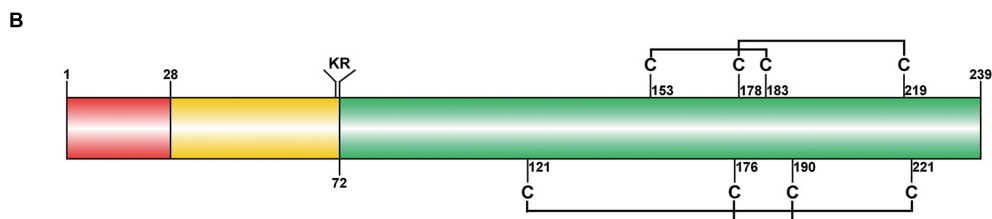| Sequence	Species	GenBank accession number
Csa-CFSH1	*Callinectes sapidus*	GU016328
Lvit-CFSH1a	*Lysmata vittata*	MT114199
Pj-CFSH2	*Penaeus japonicus*	LC224021
Sp-CFSH	*Scylla paramamosain*	MF489232

FIGURE 1 | Molecular characterization of *Lvit-CFSH1a*. **(A)** The nucleotide and deduced amino acid sequence of *Lvit-CFSH1a*. The signal peptide was shown in black box, the CFSH precursor-related peptide was in bold italics, the dibasic cleavage site (KR) was boxed in gray, the N-glycosylation motif was shown in blue background and the putative polyadenylation signal (AATAAA) is underlined. **(B)** Schematic diagram of preproprotein of *Lvit*-CFSH1a. Signal peptide (red box), CFSH precursor-related peptide (yellow box), a dibasic cleavage site KR, and the mature hormone (green box) were shown. The eight cysteine residues were predicted, and four putative disulfide bridges were connected with lines.
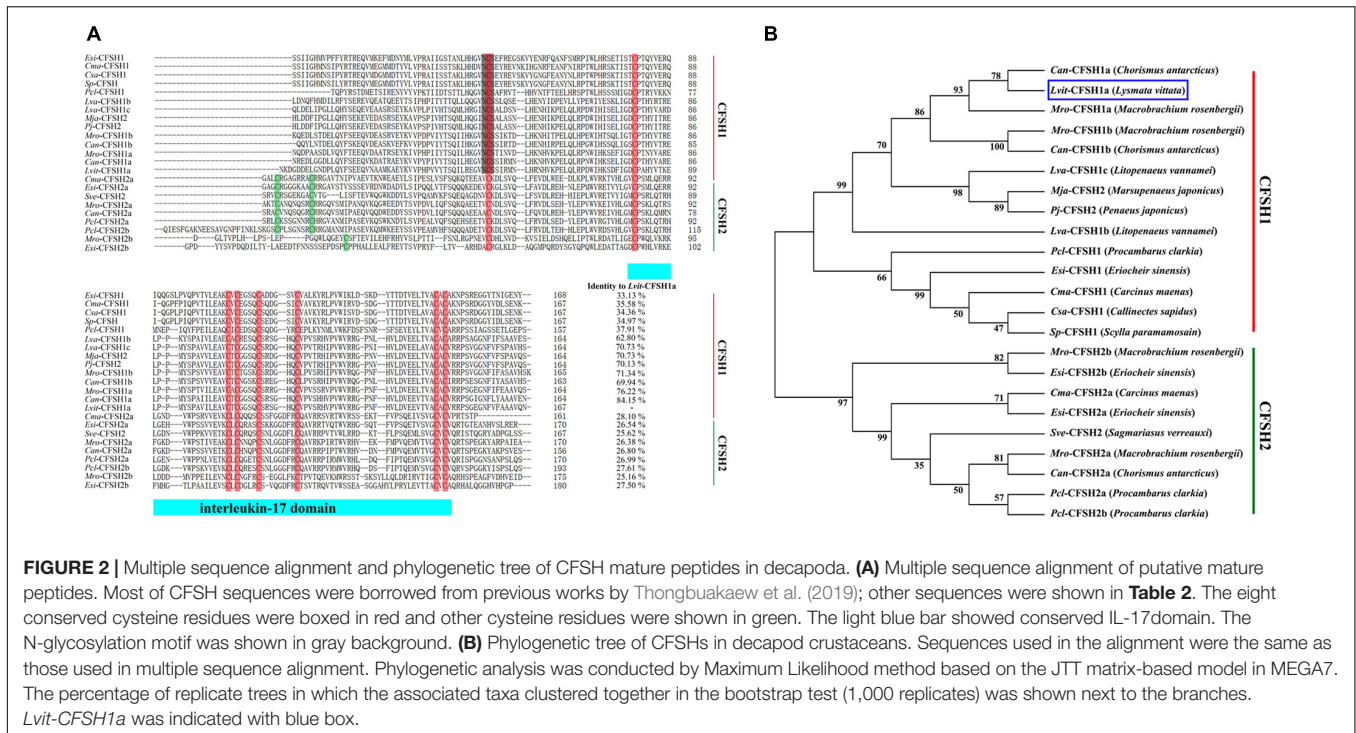
FIGURE 2 | Multiple sequence alignment and phylogenetic tree of CFSH mature peptides in decapoda. **(A)** Multiple sequence alignment of putative mature peptides. Most of CFSH sequences were borrowed from previous works by Thongbuakaew et al. (2019); other sequences were shown in **Table 2**. The eight conserved cysteine residues were boxed in red and other cysteine residues were shown in green. The light blue bar showed conserved IL-17domain. The N-glycosylation motif was shown in gray background. **(B)** Phylogenetic tree of CFSHs in decapod crustaceans. Sequences used in the alignment were the same as those used in multiple sequence alignment. Phylogenetic analysis was conducted by Maximum Likelihood method based on the JTT matrix-based model in MEGA7. The percentage of replicate trees in which the associated taxa clustered together in the bootstrap test (1,000 replicates) was shown next to the branches. Lvit-CFSH1a was indicated with blue box.
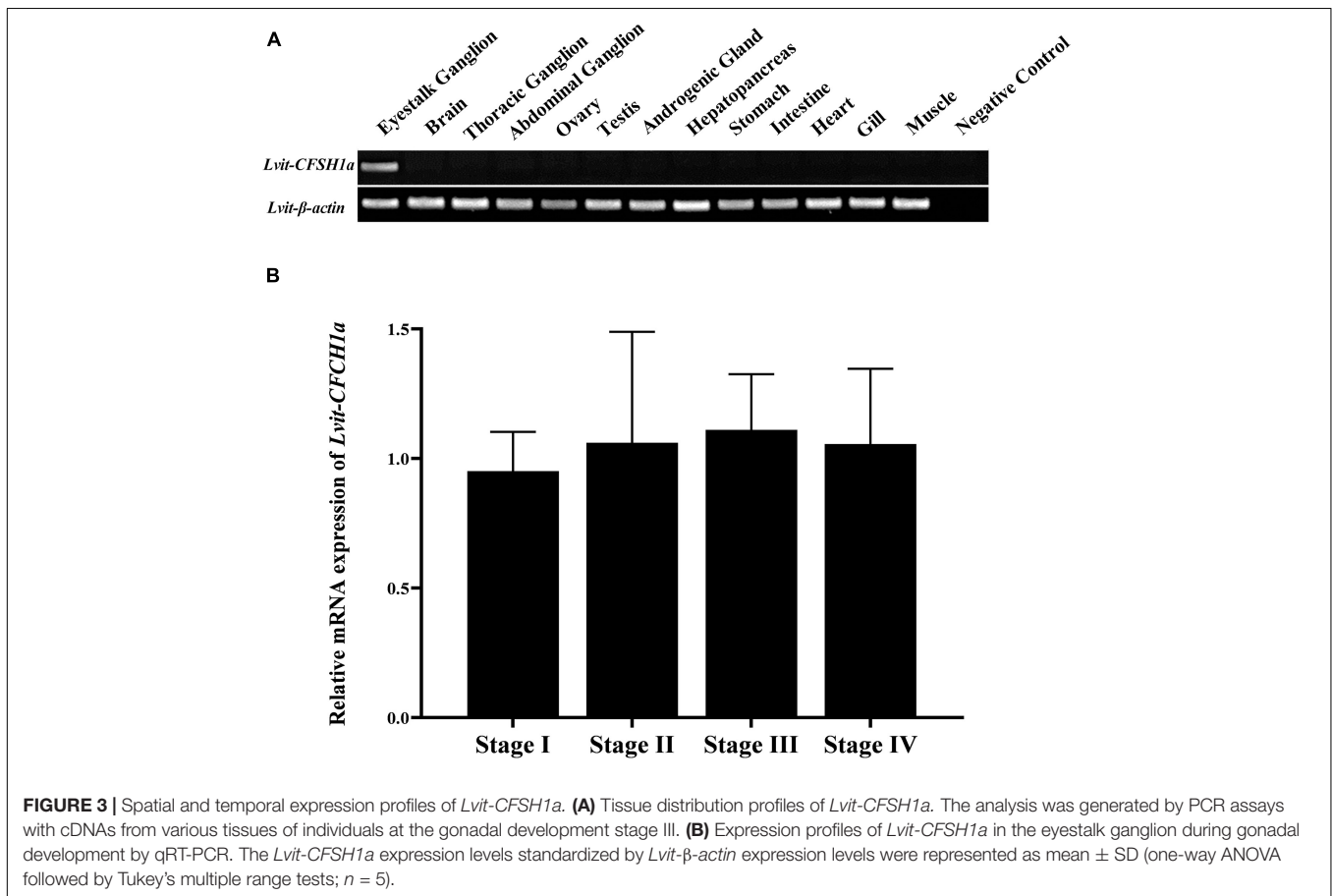
FIGURE 3 | Spatial and temporal expression profiles of Lvit-CFSH1a. **(A)** Tissue distribution profiles of Lvit-CFSH1a. The analysis was generated by PCR assays with cDNAs from various tissues of individuals at the gonadal development stage III. **(B)** Expression profiles of Lvit-CFSH1a in the eyestalk ganglion during gonadal development by qRT-PCR. The Lvit-CFSH1a expression levels standardized by Lvit-β-actin expression levels were represented as mean ± SD (one-way ANOVA followed by Tukey's multiple range tests; $n = 5$).

Statistical Analyses

Normality of data was established by the Kolmogorov-Smirnov test. All the data were presented in a normal distribution and tested for variances homogeneity by the Levene's test. All statistical analyses were performed using the SPSS 18.0 software. Statistical significance ($p < 0.05$) of data regarding *Lvit*-CFSH1a expression profile and silencing experiments was determined using one-way ANOVA followed by Tukey's multiple range tests. The *t*-test was used to analyze the data of r*Lvit*-CFSH1a injection experiment. All data were presented as mean ± SD.

RESULTS

Full Length of *Lvit-CFSH1a*

Lvit-CFSH1a (GenBank accession number: MT114199) cDNA was 1,220-bp in length with a 34-bp 5′-UTR, a 720-bp ORF, and a 467-bp 3′-UTR with a polyA tail in order (**Figure 1A**). The ORF encoded a polypeptide of 239-aa, including a 34-aa signal peptide, a 44-aa CFSH-precursor-related peptide, a dibasic processing signal (Lys-Arg), and a 161-aa mature peptide (**Figure 1**). A single polyadenylation signal ATTAAA is present in the 3′UTR of *Lvit-CFSH1a* (**Figure 1A**). Eight cysteine residues forming four disulfide bridges were found in *Lvit-CFSH1a* (**Figure 1B**). Genomic DNA of *Lvit-CFSH1a* was also cloned but no intron was found.

Homology and Phylogenetic Analysis

Multiple sequence alignment of deduced mature peptide of CFSHs was shown in **Figure 2A**. Eight conserved cysteine residues and an interleukin 17 (IL-17) domain were found in *Lvit*-CFSH1a, and that was faultlessly aligned with other CFSHs (**Figure 2A**). According to the former studies (Kotaka and Ohira, 2018; Tsutsui et al., 2018), the CFSHs were grouped into two subtypes: type I and type II. The type I CFSHs possessed a single conserved N-glycosylation motif while the type II CFSHs contained additional one or two cysteine residues (**Figure 2A**). *Lvit*-CFSH1a mature peptide shared the highest identity with *Can*-CFSH1a (84.15%).

Phylogenetic analysis demonstrated that the CFSHs in the decapod crustaceans formed two major clades: type I and type II CFSH. *Lvit*-CFSH1a was classified into type I CFSH (**Figure 2B**).

Expression Profiles of *Lvit-CFSH1a*

RT-PCR was performed on *L. vittata* at the gonadal development stage III to determine the spatial distribution profile of *Lvit-CFSH1a*. The findings were that *Lvit-CFSH1a* was exclusively expressed in the eyestalk ganglion (**Figure 3A**). The relative expression of *Lvit-CFSH1a* in the eyestalk ganglion during gonadal development was also assessed by qRT-PCR. No significant difference was observed in *Lvit-CFSH1a* expression levels during gonadal development ($F_{3,\ 16} = 0.265$, $p = 0.850$) (**Figure 3B**).

Short-Term Silencing Experiment *in vivo*

The findings revealed that in comparison to the PBS-injected treatment, transcripts of *Lvit-CFSH1a* were 83.7% inhibited [$F_{(2,}$

$_{12)} = 37.675$, $p < 0.05$]; while no significant changes in *Lvit-CFSH1b* expression levels were observed ($F_{(2,\ 12)} = 0.254$, $p = 0.780$]. Meanwhile, knockdown of *Lvit-CFSH1a* resulted in extremely significant upregulation of *Lvit-IAG2* levels [$F_{(2,\ 12)} = 115.993$, $p < 0.05$] but almost did not affect the expression levels of *Lvit-IAG1* [$F_{(2,\ 12)} = 0.008$, $p = 0.992$] (**Figure 4**).

Long-Term Silencing Experiment *in vivo*

Effects of *Lvit-CFSH1a* Silencing on Gene Expression

Compared to the PBS treatment, transcript of *Lvit-CFSH1a* was 81.7% inhibited [$F_{(2,\ 15)} = 20.686$, $p < 0.05$] (**Figure 5**). The
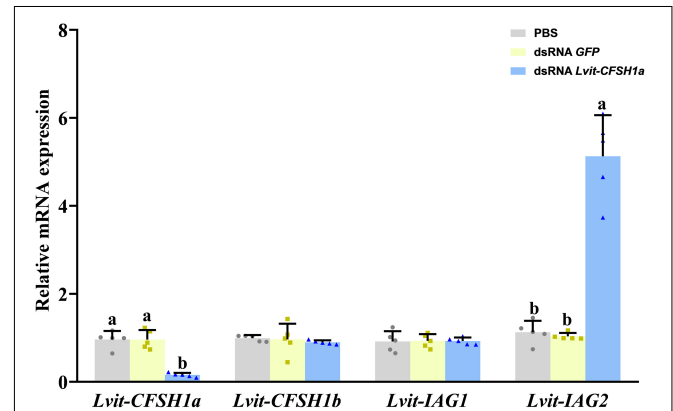

FIGURE 4 | Effects of short-term *Lvit-CFSH1a* silencing on gene expression of *L. vittata*. The efficacy of gene knockdown in the short-term *Lvit-CFSH1a* silencing experiment was evaluated by qRT-PCR. The expression levels of *Lvit-CFSH1a*, *Lvit-CFSH1b*, *Lvit-IAG1*, and *Lvit-IAG2* were detected following *in vivo* injection with PBS, dsRNA *GFP* or dsRNA *Lvit-CFSH1a*. The gene expression levels were standardized by *Lvit*-β-*actin* expression levels and represented as mean ± SD ("a and b," $p < 0.05$; one-way ANOVA followed by Tukey's multiple range tests; $n = 5$).

FIGURE 5 | Effects of long-term *Lvit-CFSH1a* silencing on gene expression of *L. vittata*. The efficacy of gene knockdown in the long-term *Lvit-CFSH1a* silencing experiment was evaluated by qRT-PCR. The expression levels of *Lvit-CFSH1a*, *Lvit-IAG1*, *Lvit-IAG2*, *Lvit-Vg*, and *Lvit-VgR* were detected following *in vivo* injection with PBS, dsRNA *GFP* or dsRNA *Lvit-CFSH1a*. The gene expression levels were standardized by *Lvit*-β-*actin* expression levels and represented as mean ± SD ("a, b and c," $p < 0.05$; one-way ANOVA followed by Tukey's multiple range tests; $n = 5$–7).
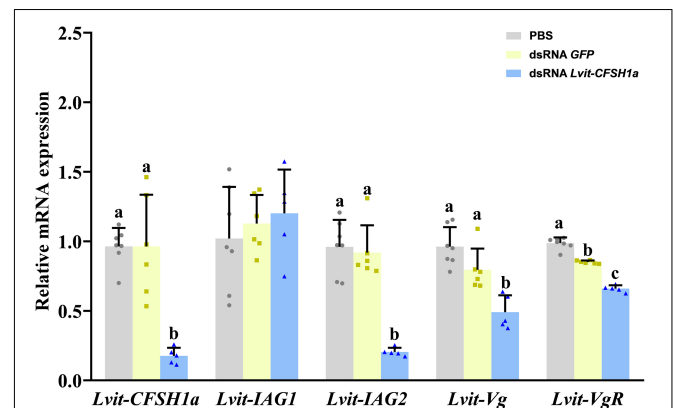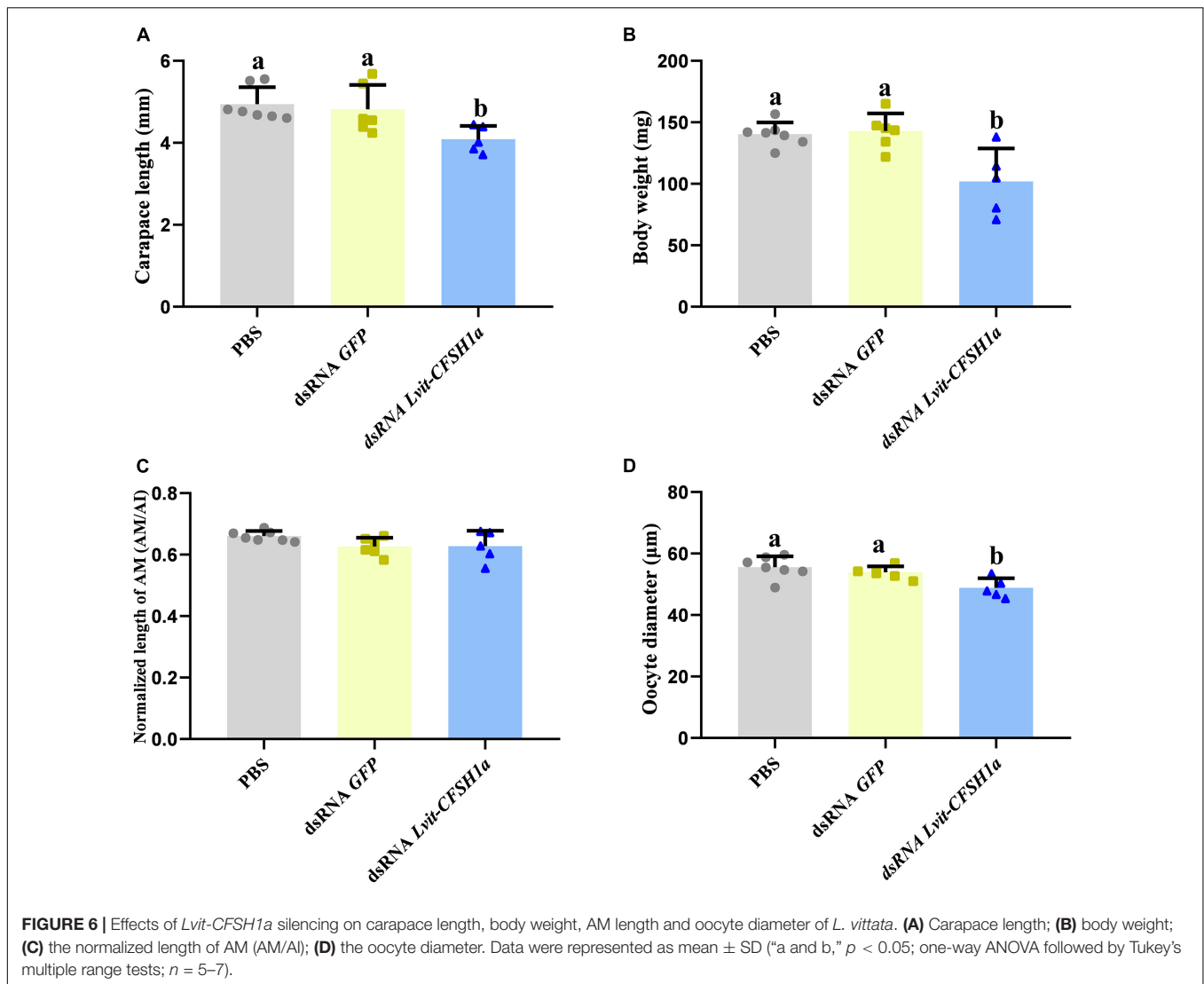
FIGURE 6 | Effects of *Lvit-CFSH1a* silencing on carapace length, body weight, AM length and oocyte diameter of *L. vittata*. **(A)** Carapace length; **(B)** body weight; **(C)** the normalized length of AM (AM/AI); **(D)** the oocyte diameter. Data were represented as mean ± SD ("a and b," $p < 0.05$; one-way ANOVA followed by Tukey's multiple range tests; n = 5–7).

relative expression of genes associated with gonadal development and sexual differentiation were also assessed by qRT-PCR. Results showed that the expression of *Lvit-IAG2* in the androgenic gland was significantly reduced [$F_{(2, 15)} = 34.597$, $p < 0.05$], but no significant difference was detected for *Lvit-IAG1* expression [$F_{(2, 15)} = 0.524$, $p = 0.603$]. Meanwhile, *Lvit-Vg* mRNA expression level in the hepatopancreas [$F_{(2, 15)} = 16.651$, $p < 0.05$] and *Lvit-VgR* mRNA expression level in the ovary [$F_{(2, 15)} = 175.194$, $p < 0.05$] were found significantly down-regulated (**Figure 5**).
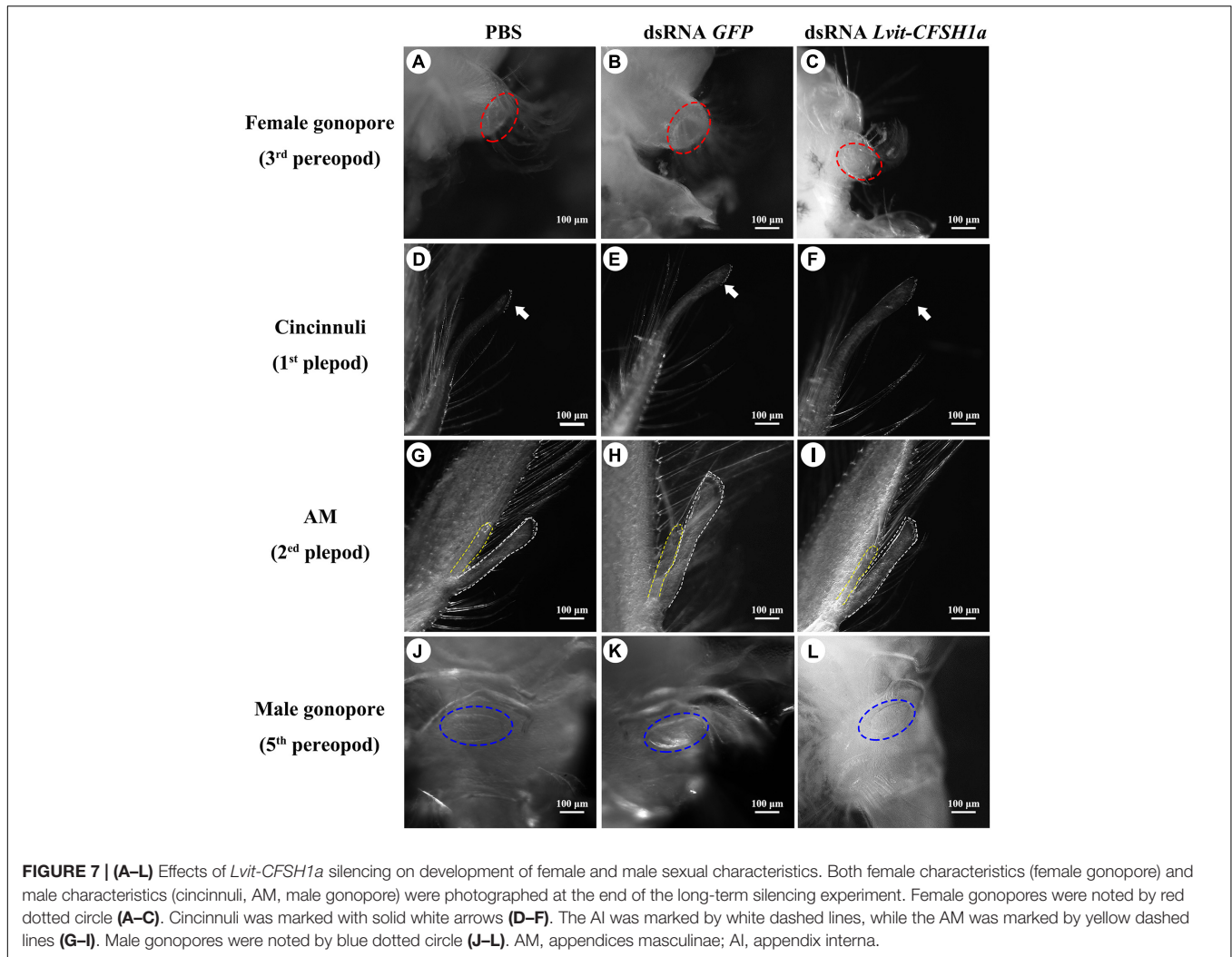
Effects of *Lvit-CFSH1a* Silencing on Growth and Development of Sexual Characteristics

At the end of the 30-day long-term trial, we recorded the average carapace length and bodyweight of the shrimps. Compared with individuals from the PBS (4.94 ± 0.06 mm, 140.36 ± 1.37 mg) or dsRNA *GFP* (4.82 ± 0.09 mm, 142.90 ± 2.05 mg) treatments, shrimps in dsRNA *Lvit-CFSH1a* (4.09 ± 0.05 mm, 101.90 ± 3.84 mg) treatment were significantly smaller [carapace length: $F_{(2, 15)} = 5.441$, $p < 0.05$; body weight: $F_{(2, 15)} = 9.124$,

$p < 0.05$] (**Figures 6A,B**). Moreover, changes in female and male sexual characteristics were also documented through photography (**Figure 7**). On the one hand, *Lvit-CFSH1a* gene knockdown led to retardation of female sexual characteristics. In the PBS and dsRNA *GFP* treatment, gonophores bulged out like a frustum surrounded by lush feathery setae (**Figures 7A,B**). Female gonophores in dsRNA *Lvit-CFSH1a* treatment were hypogenesis (**Figure 7C**). Contrary to the controls, gonophores were less visually evident or completely disappeared. The feathery setae surrounding the female gonopores located at the base of the third pair of pereiopods were substantially sparse (**Figure 7C**). On the other hand, no significant difference in male characteristics (cincinnuli, AM and male gonopore) was observed (**Figures 6C, 7D–L**).

Effects of *Lvit-CFSH1a* Silencing on Gonadal Development

Morphological and histological characteristics of gonads following *Lvit-CFSH1a* knockdown were recorded. Knockdown

FIGURE 7 | (A–L) Effects of *Lvit-CFSH1a* silencing on development of female and male sexual characteristics. Both female characteristics (female gonopore) and male characteristics (cincinnuli, AM, male gonopore) were photographed at the end of the long-term silencing experiment. Female gonopores were noted by red dotted circle **(A–C)**. Cincinnuli was marked with solid white arrows **(D–F)**. The AI was marked by white dashed lines, while the AM was marked by yellow dashed lines **(G–I)**. Male gonopores were noted by blue dotted circle **(J–L)**. AM, appendices masculinae; AI, appendix interna.

of *Lvit-CFSH1a* led to retardation of ovarian region. In dsRNA *Lvit-CFSH1a* treatment, the ovarian region was thinner (**Figure 8C**). Additionally, the oocyte size significantly decreased following injection of dsRNA *Lvit-CFSH1a* (**Figures 6D, 8D–F**). For the PBS and dsRNA *GFP* treatment, the average oocyte diameter was $55.57 \pm 0.51\ \mu m$ ($n = 7$) and $53.87 \pm 0.28\ \mu m$ ($n = 6$), respectively. Following knockdown of *Lvit-CFSH1a*, the oocyte diameter decreased to $48.81 \pm 0.46\ \mu m$ ($n = 5$). However, *Lvit-CFSH1a* knockdown had no significant effect on testicular development. Testicular regions of the three treatments were cloudy white (**Figures 8A–C**). Gonadal histology further showed that similar compositions of germ cell types were observed among the three treatments. Abundant of spermatocytes I (Sc I), spermatid (Sd), and spermatozoa (Sz) were found in the testicular region of the three treatments (**Figures 8G–I**).

In vivo Effect of *rLvit-CFSH1a* on Gene Expression

To determine the effect of *Lvit*-CFSH1a on *Lvit-IAG1*, *Lvit-IAG1*, *Lvit-Vg*, and *Lvit-VgR*, two experimental groups were injected

with either r*Lvit*-CFSH1a or carrier only (PBS). The findings revealed that injection of r*Lvit*-CFSH1a resulted in extremely significant downregulation of *Lvit-IAG2* levels ($p = 0.0028$) but almost did not affect the expression levels of *Lvit-IAG1*, *Lvit-Vg*, and *Lvit-VgR* (**Figure 9**).

DISCUSSION

CFSH is a crucial hormone involved in development of female-related phenotypes in dioecious crustaceans (Zmora and Chung, 2014; Jiang et al., 2020). However, the biological functions of CFSH in PSH crustaceans have been rarely investigated.

In our current study, we established a transcript of CFSH (*Lvit-CFSH1a*) in the PSH shrimp, *L. vittata*. By cloning of *Lvit-CFSH1a* gDNA sequence, we confirmed that transcripts of *Lvit-CFSH1a* and *Lvit-CFSH1b* were derived from different genes. Though abundant of nuclear sequence of CFSHs were reported in decapod crustaceans, to date, only two type I CFSHs, *Csa*-CFSH1 (*Callinectes sapidus*), and *Sp*-CFSH (*Scylla paramamosain*), have been proved to stimulate female sexual
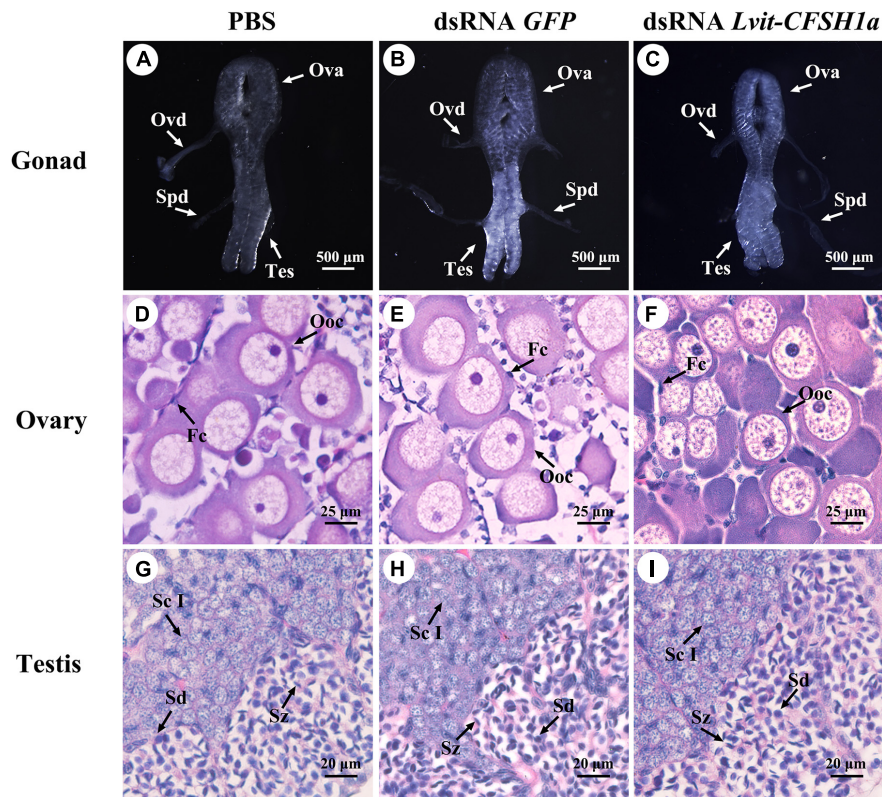
FIGURE 8 | Effects of *Lvit-CFSH1a* silencing on gonadal development of *L. vittata*. Gonad morphology and characteristics were photographed following *in vivo* injection of PBS **(A)**, dsRNA *GFP* **(B)** or dsRNA *Lvit-CFSH1a* **(C)**. Hematoxylin and eosin (H&E)-stained sections was used for follow-up structure description of ovarian region **(D–F)** and testicular region **(G–I)**. Ova, ovary; Tes, testis; Ovd, oviduct; Spd, sperm duct; Ooc, oocytes; Fc, follicular cell; Sc I, primary spermatocyte; Sd, spermatid; Sz, spermatozoa.

differentiation (Ventura et al., 2014; Zmora and Chung, 2014; Veenstra, 2015, 2016; Nguyen et al., 2016; Kotaka and Ohira, 2018; Liu et al., 2018; Tsutsui et al., 2018; Thongbuakaew et al., 2019; Jiang et al., 2020). While expression of CFSH transcripts were detected in a variety of tissues (Veenstra, 2015; Nguyen et al., 2016; Tsutsui et al., 2018; Thongbuakaew et al., 2019), *Csa*-CFSH1 and *Sp*-CFSH were exclusively expressed in the eyestalk ganglion (Zmora and Chung, 2014; Jiang et al., 2020). In this study, *Lvit*-CFSH1a shared similar characteristics with other type I CFSHs (Kotaka and Ohira, 2018; Tsutsui et al., 2018). Phylogenetic tree analysis further demonstrated that *Lvit*-CFSH1a was classified into type I CFSH. Besides, *Lvit*-CFSH1a was also exclusively expressed in the eyestalk ganglion, which was consistent with studies in *C. sapidus* and *S. paramamosain* (Zmora and Chung, 2014; Jiang et al., 2020). Thus, *Lvit*-CFSH1a was possibly involved in development of female-related phenotypes of the PSH species. Alternatively, the constant and stable expression of *Lvit*-CFSH1a during the life cycle of the PSH species suggested that *Lvit*-CFSH1a might not participate in gonad development.

Our findings revealed that RNAi induced a specific knockdown of the *Lvit-CFSH1a* transcripts level by 83.7% in a short-term experiment, and by 81.7% in a long-term experiment. Furthermore, we assessed the influence of *Lvit*-CFSH1a on the development of female features by comparing
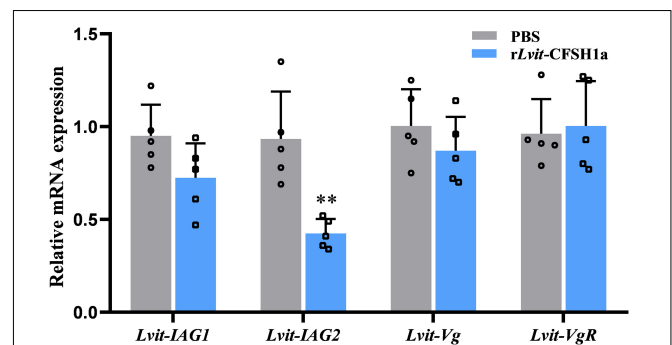

FIGURE 9 | Effects of r*Lvit-CFSH1a* on gene expression of *L. vittata* in vivo. The expression levels of *Lvit-IAG1*, *Lvit-IAG2*, *Lvit-Vg*, and *Lvit-VgR* were detected following *in vivo* injection with PBS or r*Lvit-CFSH1a*. The gene expression levels were standardized by *Lvit-β-actin* expression levels and represented as mean ± SD (*t*-test, with **$p < 0.01$; $n = 5$).

female external features and ovarian development status. In the present study, we found that *Lvit-CFSH1a* gene knockdown led to retardation of female sexual characteristics. Numbers of feathery setae surrounding the female gonopores were substantially sparse. This result is similar to those described in *C. sapidus* and *S. paramamosain* (Zmora and Chung, 2014;

Jiang et al., 2020). However, results varied when it came to the influences on ovarian development. In fact, to date the effect of CFSH on ovarian development remains obscure. In *C. sapidus*, knockdown of *Cs-CFSH* showed no significant effect on the ovarian development (Zmora and Chung, 2014). Study in *M. japonicus* suggested that CFSH might participate in some reproductive process other than vitellogenesis (Tsutsui et al., 2018). Research in *M. rosenbergii* also demonstrated that both type I and type II CFSHs had unknown effect on ovarian development (Thongbuakaew et al., 2019). In the present study, a repression phenomenon was observed in the ovarian region of *L. vittata* in long-term silencing experiment. Contrary to the controls, ovarian region in the *Lvit-CFSH1a* silencing treatment was less developed with significantly smaller oocytes. Moreover, qRT-PCR data lent support to histomorphological results. It is known that both the *Vg* gene expression levels in hepatopancreas and *VgR* gene expression levels in ovary are approved indexes of ovarian development (Warrier and Subramoniam, 2002; Subramoniam, 2011; Jia et al., 2013; Urtgam et al., 2015). Following *Lvit-CFSH1a* knockdown, *Lvit-Vg* expression in the hepatopancreas and *Lvit-VgR* expression in the ovary were found significantly down-regulated. It seemed plausible that *Lvit*-CFSH1a stimulated ovarian development via promoting vitellogenesis. We also purified *Lvit*-CFSH1a mature peptide and conducted a further *in vivo* injection experiment in the study. However, results of r*Lvit*-CFSH1a administration demonstrated that r*Lvit*-CFSH1a affect neither vitellogenin synthesis in the hepatopancreas nor vitellogenesis in the gonad. Moreover, no significant difference was observed in *Lvit-CFSH1a* expression levels during gonadal development (**Figure 3**). These results jointly suggested that *Lvit*-CFSH1a might regulate ovarian development via some unknown process other than vitellogenesis. It is worth noting that, as shown in **Figures 6A,B**, *Lvit-CFSH1a* silencing induced significantly slower growth in the treated shrimps. It is known that growth and reproduction are closely related, gonadal development and fecundity usually increase with body size (Heino and Kaitala, 2001; Michalakis et al., 2013). The same phenomenon has also been observed in *L. vittata* (Chen et al., 2019). Thus, another possibility is that long-term *Lvit-CFSH1a* silencing caused significantly slower growth in the treated shrimps and this indirectly hindered the ovarian development, along with smaller oocytes and down-regulation of *Lvit-Vg* and *Lvit-VgR* expression.

Simultaneously, we evaluated the effects of *Lvit*-CFSH1a on male development in the study. In *S. paramamosain*, it was reported that CFSH acts as an inhibitor of IAG (Liu et al., 2018). In dioecious decapod crustaceans, there is usually one IAG gene in a species (Li et al., 2012; Chung, 2014; Huang et al., 2017). Transcripts generated by alternative splicing of the same IAG gene have different functions in different organs (Li et al., 2012; Chung, 2014; Huang et al., 2017). Nevertheless, two IAG genes were identified in the PSH shrimp *L. vittata*, and they cooperatively modulated male sexual differentiation of the species (Liu et al., 2021a,b). Specifically, *Lvit*-IAG1 was suggested to be closely related to the development of both AM and male gonopores, and participated in primary-to-secondary spermatocyte transition (Liu et al., 2021b); whereas

Lvit-IAG2 was somewhat related to the development of AM, and participated in secondary spermatocyte-to-spermatid transition (Liu et al., 2021a). In the present study, results of short-term silencing experiment and r*Lvit*-CFSH1a injection experiment demonstrated that *Lvit*-CFSH1a acted as an inhibitor of *Lvit*-IAG2 rather than *Lvit*-IAG1. Thus, we speculated that knockdown of *Lvit-CFSH1a* might slightly stimulate male sexual differentiation in long-term silencing experiment, such as relatively longer AM and more spermatid/spermatozoa in the testicular regions. However, at the end of the 30-day long-term trial, no significant promotion in male sexual differentiation was observed. Long-term *Lvit-CFSH1a* knockdown affected neither testicular maturation nor development of male-related phenotypes. Notably, *Lvit-IAG2* expression was significantly suppressed, which was contradictory to the above hypothesis. The following may explain these apparently contradictory results. Previous studies suggested that *Lvit*-IAG2 is more than a sexual differentiation regulator, and it also stimulates the growth of the PSH species (Liu et al., 2021a). In the present study, silencing the *Lvit-CFSH1a* gene impeded individual growth of the species. Moreover, no significant difference was observed in *Lvit-CFSH1a* expression levels during the life cycle of the PSH species (**Figure 3**). Based on the above results, we proposed that *Lvit*-CFSH1a might involve some unknown biological processes and ultimately influence individual growth. In the short-term trial (**Figures 4, 9**), *Lvit-IAG2* expression was significantly suppressed by *Lvit*-CFSH1a, but in the long-term experiment the adverse effects of *Lvit*-CFSH1a silencing on growth became more obvious (**Figure 6**), and it in turn affected expression of growth-related gene (e.g., *Lvit*-IAG2). With the decrease of *Lvit*-IAG2, the rate of male differentiation in dsRNA *Lvit-CFSH1a* treatment was slower than the PBS or dsRNA *GFP* treatment, which eventually led to similar development of male-related phenotypes among the three treatments.

In summary, we characterized a CFSH gene, *Lvit-CFSH1a*, from the eyestalk ganglion of the PSH species *L. vittata*. This study showed that *Lvit*-CFSH1a regulated female-related phenotypes, but didn't evidently affect the male sexual differentiation. In addition, *Lvit*-CFSH1a might participate in the regulation of individual growth.

DATA AVAILABILITY STATEMENT

The datasets presented in this study can be found in online repositories. The names of the repository/repositories and accession number(s) can be found in the article/**Supplementary Material**.

AUTHOR CONTRIBUTIONS

FL contributed to conceptualization, methodology, software, validation, formal analysis, investigation, data curation, visualization, and writing—original draft preparation of the study. HY contributed to conceptualization, methodology, validation, data curation, writing—review and editing,

SUPPLEMENTARY MATERIAL

The Supplementary Material for this article can be found online at: https://www.frontiersin.org/articles/10.3389/fmars.2021.791965/full#supplementary-material

REFERENCES

Alves, D. F. R., Greco, L. S. L., Barros-Alves, S. D., and Hirose, G. L. (2019). Sexual system, reproductive cycle and embryonic development of the red-striped shrimp *Lysmata vittata*, an invader in the western Atlantic Ocean. *PLoS One* 14:e0210723. doi: 10.1371/journal.pone.0210723

Bao, C. C., Liu, F., Yang, Y. A., Lin, Q., and Ye, H. H. (2020). Identification of peptides and their GPCRs in the peppermint shrimp *Lysmata vittata*, a protandric simultaneous hermaphrodite species. *Front. Endocrinol.* 11:226. doi: 10.3389/fendo.2020.00226

Barki, A., Karplus, I., Khalaila, I., Manor, R., and Sagi, A. (2003). Male-like behavioral patterns and physiological alterations induced by androgenic gland implantation in female crayfish. *J. Exp. Biol.* 206(Pt 11), 1791–1797. doi: 10.1242/jeb.00335

Barki, A., Karplus, I., Manor, R., and Sagi, A. (2006). Intersexuality and behavior in crayfish: the de-masculinization effects of androgenic gland ablation. *Horm. Behav.* 50, 322–331. doi: 10.1016/j.yhbeh.2006.03.017

Bauer, R. T. (2000). Simultaneous hermaphroditism in caridean shrimps: a unique and puzzling sexual system in the Decapoda. *J. Crustacean Biol.* 20, 116–128. doi: 10.1163/1937240x-90000014

Bornhorst, J. A., and Falke, J. J. (2000). Purification of proteins using polyhistidine affinity tags. *Methods Enzymol.* 326, 245–254. doi: 10.1016/s0076-6879(00)26058-26058

Chen, D. M., Liu, F., Zhu, Z. H., Lin, Q., Zeng, C. S., and Ye, H. H. (2019). Ontogenetic development of gonads and external sexual characters of the protandric simultaneous hermaphrodite peppermint shrimp, *Lysmata vittata* (Caridea: Hippolytidae). *PLoS One* 14:e0215406. doi: 10.1371/journal.pone.0215406

Chung, J. S. (2014). An insulin-like growth factor found in hepatopancreas implicates carbohydrate metabolism of the blue crab *Callinectes sapidus*. *Gen. Comp. Endocrinol.* 199, 56–64. doi: 10.1016/j.ygcen.2014.01.012

Fu, C. P., Li, F. J., Wang, L. F., Wu, F. R., Wang, J. M., Fan, X. L., et al. (2020). Molecular characteristics and abundance of insulin-like androgenic gland hormone and effects of RNA interference in *Eriocheir sinensis*. *Anim. Reprod. Sci.* 215:106332. doi: 10.1016/j.anireprosci.2020.106332

Heino, M., and Kaitala, V. (2001). Evolution of resource allocation between growth and reproduction in animals with indeterminate growth. *J. Evol. Biol.* 12, 423–429. doi: 10.1046/j.1420-9101.1999.00044.x

Huang, X. S., Ye, H. H., and Chung, J. S. (2017). The presence of an insulin-like androgenic gland factor (IAG) and insulin-like peptide binding protein (ILPBP) in the ovary of the blue crab, *Callinectes sapidus* and their roles in ovarian development. *Gen. Comp. Endocrinol.* 249, 64–70. doi: 10.1016/j.ygcen.2017.05.001

Jia, X. W., Chen, Y. D., Zou, Z. H., Lin, P., Wang, Y. L., and Zhang, Z. P. (2013). Characterization and expression profile of vitellogenin gene from *Scylla paramamosain*. *Gene.* 520, 119–130. doi: 10.1016/j.gene.2013.02.035

Jiang, Q. L., Lu, B., Lin, D. D., Huang, H. Y., Chen, X. L., and Ye, H. H. (2020). Role of crustacean female sex hormone (CFSH) in sex differentiation in early juvenile mud crabs, *Scylla paramamosain*. *Gen. Comp. Endocrinol.* 289:113383. doi: 10.1016/j.ygcen.2019.113383

Juchault, P. (1999). Hermaphroditism and gonochorism. A new hypothesis on the evolution of sexuality in *Crustacea*. *C. R. Acad. Sci. III Sci. Vie.* 322, 423–427. doi: 10.1016/s0764-4469(99)80078-x

Khalaila, I., Katz, T., Abdu, U., Yehezkel, G., and Sagi, A. (2001). Effects of implantation of hypertrophied androgenic glands on sexual characters and physiology of the reproductive system in the female red claw crayfish, *Cherax quadricarinatus*. *Gen. Comp. Endocrinol.* 121, 242–249. doi: 10.1006/gcen.2001.7607

Kotaka, S., and Ohira, T. (2018). cDNA cloning and in situ localization of a crustacean female sex hormone-like molecule in the kuruma prawn *Marsupenaeus japonicus*. *Fish. Sci.* 84, 53–60. doi: 10.1007/s12562-017-1152-1157

Levy, T., and Sagi, A. (2020). The "IAG-Switch"-A key controlling element in decapod crustacean sex differentiation. *Front. Endocrinol.* 11:651. doi: 10.3389/fendo.2020.00651

Levy, T., Tamone, S. L., Manor, R., Aflalo, E. D., Sklarz, M. Y., Chalifa-Caspi, V., et al. (2020). The IAG-switch and further transcriptomic insights into sexual differentiation of a protandric shrimp. *Front. Mar. Sci.* 7:587454. doi: 10.3389/fmars.2020.587454

Li, S. H., Li, F. H., Sun, Z., and Xiang, J. H. (2012). Two spliced variants of insulin-like androgenic gland hormone gene in the Chinese shrimp, *Fenneropenaeus chinensis*. *Gen. Comp. Endocrinol.* 177, 246–255. doi: 10.1016/j.ygcen.2012.04.010

Liu, A., Liu, J., Liu, F., Huang, Y. Y., Wang, G. Z., and Ye, H. H. (2018). Crustacean female sex hormone from the mud crab *Scylla paramamosain* is highly expressed in prepubertal males and inhibits the development of androgenic gland. *Front. Physiol.* 9:924. doi: 10.3389/fphys.2018.00924

Liu, F., Shi, W. Y., Ye, H. H., Liu, A., and Zhu, Z. H. (2021a). RNAi reveals role of insulin-like androgenic gland hormone 2 (IAG2) in sexual differentiation and growth in hermaphrodite shrimp. *Front. Mar. Sci.* 8:666763. doi: 10.3389/fmars.2021.666763

Liu, F., Shi, W. Y., Ye, H. H., Zeng, C. S., and Zhu, Z. H. (2021b). Insulin-like androgenic gland hormone 1 (IAG1) regulates sexual differentiation in a hermaphrodite shrimp through feedback to neuroendocrine factors. *Gen. Comp. Endocrinol.* 303:113706. doi: 10.1016/j.ygcen.2020.113706

Malecha, S. R., Nevin, P. A., Ha, P., Barck, L. E., Lamadridrose, Y., Masuno, S., et al. (1992). Sex-ratios and sex-determination in progeny from crosses of surgically sex-reversed fresh-water prawns, *Macrobrachium rosenbergii*. *Aquaculture* 105, 201–218. doi: 10.1016/0044-8486(92)90087-90082

Manor, R., Weil, S., Oren, S., Glazer, L., Aflalo, E. D., Ventura, T., et al. (2007). Insulin and gender: an insulin-like gene expressed exclusively in the androgenic gland of the male crayfish. *Gen. Comp. Endocrinol.* 150, 326–336. doi: 10.1016/j.ygcen.2006.09.006

Michalakis, K., Mintziori, G., Kaprara, A., Tarlatzis, B. C., and Goulis, D. G. (2013). The complex interaction between obesity, metabolic syndrome and reproductive axis: a narrative review. *Metab. Clin. Exp.* 62, 457–478. doi: 10.1016/j.metabol.2012.08.012

Nagamine, C., Knight, A. W., Maggenti, A., and Paxman, G. (1980). Masculinization of female *Macrobrachium rosenbergii* (de Man) (Decapoda, Palaemonidae) by androgenic gland implantation. *Gen. Comp. Endocrinol.* 41, 442–457. doi: 10.1016/0016-6480(80)90049-90040

Nguyen, T. V., Cummins, S. F., Elizur, A., and Ventura, T. (2016). Transcriptomic characterization and curation of candidate neuropeptides regulating reproduction in the eyestalk ganglia of the *Australian crayfish*, *Cherax quadricarinatus*. *Sci. Rep.* 6:38658. doi: 10.1038/srep38658

Rosen, O., Manor, R., Weil, S., Gafni, O., Linial, A., Aflalo, E. D., et al. (2010). A sexual shift induced by silencing of a single insulin-like gene in crayfish: ovarian upregulation and testicular degeneration. *PLoS One* 5:e15281. doi: 10.1371/journal.pone.0015281

Shi, W. Y., Liu, F., Liu, A., Huang, H. H., Lin, Q., Zeng, C. S., et al. (2020). Roles of gonad-inhibiting hormone in the protandric simultaneous hermaphrodite peppermint shrimp. *Biol. Reprod.* 103, 817–827. doi: 10.1093/biolre/ioaa111

Subramoniam, T. (2011). Mechanisms and control of vitellogenesis in crustaceans. *Fish. Sci.* 77, 1–21. doi: 10.1007/s12562-010-0301-z

Taketomi, Y., and Nishikawa, S. (1996). Implantation of androgenic glands into immature female crayfish, *Procambarus clarkii*, with masculinization of sexual characteristics. *J. Crustacean Biol.* 16, 232–239. doi: 10.1163/193724096X00027

Thongbuakaew, T., Suwansa-ard, S., Sretarugsa, P., Sobhon, P., and Cummins, S. F. (2019). Identification and characterization of a crustacean female sex hormone in the giant freshwater prawn, *Macrobrachium rosenbergii*. *Aquaculture* 507, 56–68. doi: 10.1016/j.aquaculture.2019.04.002

Tsutsui, N., Kotaka, S., Ohira, T., and Sakamoto, T. (2018). Characterization of distinct ovarian isoform of crustacean female sex hormone in the kuruma prawn *Marsupenaeus japonicus*. *Comp. Biochem. Physiol. A Mol. Integr. Physiol.* 217, 7–16. doi: 10.1016/j.cbpa.2017.12.009

Urtgam, S., Treerattrakool, S., Roytrakul, S., Wongtripop, S., Prommoon, J., Panyima, S., et al. (2015). Correlation between gonad-inhibiting hormone and vitellogenin during ovarian maturation in the domesticated *Penaeus monodon*. *Aquaculture* 437, 1–9. doi: 10.1016/j.aquaculture.2014.11.014

Veenstra, J. A. (2015). The power of next-generation sequencing as illustrated by the neuropeptidome of the crayfish *Procambarus clarkii*. *Gen. Comp. Endocrinol.* 224, 84–95. doi: 10.1016/j.ygcen.2015.06.013

Veenstra, J. A. (2016). Similarities between decapod and insect neuropeptidomes. *PeerJ* 4:e2043. doi: 10.7717/peerj.2043

Ventura, T., Cummins, S. F., Fitzgibbon, Q., Battaglene, S., and Elizur, A. (2014). Analysis of the central nervous system transcriptome of the eastern rock lobster *Sagmariasus verreauxi* reveals its putative neuropeptidome. *PLoS One* 9:e97323. doi: 10.1371/journal.pone.0097323

Ventura, T., Manor, R., Aflalo, E. D., Weil, S., Raviv, S., Glazer, L., et al. (2009). Temporal silencing of an androgenic gland-specific insulin-like gene affecting phenotypical gender differences and spermatogenesis. *Endocrinology* 150, 1278–1286. doi: 10.1210/en.2008-2906

Warrier, S., and Subramoniam, T. (2002). Receptor mediated yolk protein uptake in the crab *Scylla serrata*: crustacean vitellogenin receptor recognizes related mammalian serum lipoproteins. *Mol. Reprod. Dev.* 61, 536–548. doi: 10.1002/mrd.10106

Zhang, D., Sun, M., and Liu, X. (2017). Phase-specific expression of an insulin-like androgenic gland factor in a marine shrimp *Lysmata wurdemanni*: implication for maintaining protandric simultaneous hermaphroditism. *PLoS One* 12:e0172782. doi: 10.1371/journal.pone.0172782

Zmora, N., and Chung, J. S. (2014). A novel hormone is required for the development of reproductive phenotypes in adult female crabs. *Endocrinology* 155, 230–239. doi: 10.1210/en.2013-1603